

Efficient genome editing in the mouse brain by local delivery of engineered Cas9 ribonucleoprotein complexes

Brett T. Staahl¹, Madhurima Benekareddy², Claire Coulon-Bainier², Ashwin A. Banfal¹, Stephen N. Floor¹, Jennifer K. Sabo¹, Cole Urnes¹, Gabriela Acevedo Munares¹, Anirvan Ghosh^{2,3}, Jennifer A. Doudna^{1,4,5,6,7,*}

¹Department of Molecular and Cell Biology, University of California, Berkeley, California, USA.

²Roche Pharma Research and Early Development, Basel, Switzerland. ³E-Scape Bio, San Francisco, California, USA. ⁴Howard Hughes Medical Institute, University of California, Berkeley, California, USA. ⁵Innovative Genomics Institute, University of California, Berkeley, California, USA. ⁶MBIB Division, Lawrence Berkeley National Laboratory, Berkeley, California, USA.

⁷Department of Chemistry, University of California, Berkeley, California, USA.

Abstract

We demonstrate editing of post-mitotic neurons in the adult mouse brain following injection of Cas9 ribonucleoprotein (RNP) complexes in the hippocampus, striatum and cortex. Engineered variants of Cas9 with multiple SV40 nuclear localization sequences enabled a ten-fold increase in the efficiency of neuronal editing *in vivo*. These advances indicate the potential of genome editing in the brain to eliminate the genetic causes of neurological diseases.

Cas9 is an RNA-guided, DNA-binding and cleaving protein that enables facile modification or perturbation of genes and non-coding genetic elements in a wide variety of organisms^{1–4}. Cas9-mediated genome editing has been used to treat diseases of the eye, ear, liver and muscle in animals, but the challenge of tissue-specific delivery remains to be addressed^{5–10}. *In vivo* delivery of genetically encoded Cas9 with viral vectors and plasmids is undesirable for several reasons, including potential direct integration into genomic DNA, immune responses elicited by persistent expression of the bacterial Cas9 protein in edited cells¹¹ and off-target editing¹². Delivery of non-genetically encoded, preassembled and short-lived Cas9 ribonucleoprotein (RNP) complexes overcomes these concerns^{5,13–16}.

*To whom correspondence should be addressed.: doudna@berkeley.edu.

Author Contributions

B.T.S., A.G. and J.A.D. conceived the study and analyzed the data. B.T.S., J.K.S., C.U., S.N.F. and G.A.M. conducted *in vitro* studies. B.T.S. did Cas9 protein and sgRNA design and RNP assembly. B.T.S. and A.B. conducted protein production. M.B., C.C.B. B.T.S. and J.K.S. conducted *in vivo* studies. B.T.S., M.B., A.G. and J.A.D. wrote the manuscript.

Competing financial interests

The authors have submitted a patent disclosure on this work. J.A.D. is employed by HHMI and works at the University at California Berkeley. UC Berkeley and HHMI have patents pending for CRISPR technologies on which she is an inventor. J.A.D. is the executive director of the Innovative Genomics Institute at UC Berkeley and UCSF. J.A.D. is a co-founder of Editas Medicine, Intellia Therapeutics and Caribou Biosciences and a scientific advisor to Caribou, Intellia, eFFECTOR Therapeutics and Driver.

To test the activity of Cas9 RNPs *in vivo* we first adapted the Ai9 tdTomato mouse to report Cas9 editing (Supplementary Fig. 1a). This reporter mouse model provides a high-throughput and quantitative readout of site-specific genome editing that results in a red fluorescent protein gain-of-signal in genetically modified cells¹⁷. We developed a sgRNA, termed sgRNAtdTom, to delete the STOP cassette and activate tdTomato expression in cells (Supplementary Fig. 1 and 2a). Upon nucleofection of neural progenitor cells (NPCs) with Cas9–2xNLS;sgRNAtdTom RNP complexes we observed a RNP dose-dependent activation of tdTomato by microscopy and flow cytometry analysis (Fig. 1a). NexGen sequence analysis (NGS) of the locus confirmed Cas9 RNP-induced insertion/deletion (indel) mutations (Supplementary Fig. 2b). PCR analysis of genomic DNA from the edited tdTomato STOP cassette revealed a DNA laddering pattern, and FACS sorting followed by genomicDNA PCR analysis showed tdTomato reporter activation requires a specific double deletion (Supplementary Fig. 2c). Sanger sequencing of the other edited alleles identified additional edits that do not activate tdTomato (Supplementary Fig. 2d, 2e). Quantification of the double deletion PCR band correlates closely with %tdTomato⁺ cells measured by flow cytometry. Therefore, although the number of tdTomato⁺ cells under-reports RNP total editing, the tdTomato mouse can be used to visually detect genome editing by Cas9 RNPs, and should enable visualization of edited cells *in vivo*.

Cas9 RNP has no innate cell penetrating activity, and its direct delivery into cells required chemical conjugation of poly-arginine peptides, a strategy prone to inefficiency and heterogeneity¹⁸, or mixing with lipid carrier molecules^{5,16} which are immunogenic, inflammatory and toxic^{19,20}. In previous work, arrays of Simian vacuolating virus 40 nuclear localization sequence (SV40-NLS) enhanced the innate cell penetrating capabilities of zinc finger nucleases²¹. The Cas9 protein we use for cell-based experiments contains two SV40 NLSs on the C-terminus, Cas9–2xNLS. However we found that RNPs generated using this protein are not cell-penetrating and do not result in genome editing when added directly to the media of cultured cells (even in the absence of serum). To test potential cell penetrating properties we designed Cas9 proteins with increasing numbers of N-terminal SV40 NLS arrays that we call 0x, 1x, 2x, 4x and 7xNLS-Cas9–2xNLS (Supplementary Table 1). These were made with and without superfolder(sf)GFP²² fused on the C-terminus (Fig. 1c). We delivered RNPs to the media of tdTomato NPC cultures. TdTomato reporter activation increased markedly with increased numbers of N-terminal NLS sequences on Cas9 and decreased for 7xNLS-Cas9–2xNLS (Fig. 1d). TdTomato was not detected with a non-targeting sgRNA. PCR analysis of tdTomato locus confirmed the expected laddering pattern indicating deletion edits and, as anticipated, showed higher total deletion efficiency than reported by %tdTomato⁺ cells (Fig. 1e).

We bypassed the requirement for protein-based cell penetration by mixing RNPs with Lipofectamine2000 to trigger RNP delivery into the cytoplasm by cell membrane fusion in HEK293 with a GFP reporter⁵ or by using a NaCl hypertonic protein transduction protocol in tdTomato NPCs²³ and observed gene editing in both cell types and editing activity was not significantly different between RNP variants at all RNP doses delivered (HEK293 $p = 0.9032$ and tdTomato NPCs $p = 0.8685$)(Supplementary Fig. 3a,b). Direct delivery of 4xNLS-Cas9–2xNLS but not 0xNLS-Cas9–2xNLS RNP triggered genome editing in mature neurons (Supplementary Fig. 3c) but when RNPs were mixed with Lipofectamine2000, both

triggered genome editing (Supplementary Fig. 3d). Together these results support our hypothesis that 4xNLS-Cas9–2xNLS have enhanced cell penetration capabilities.

We next tested the activity of the 4xNLS-Cas9–2xNLS and 0xNLS-Cas9–2xNLS RNPs in adult tdTomato mouse brains using an intracranial RNP injection system. To test RNP activity in diverse neuronal subtypes, we performed stereotaxic injections (4pmol per 0.5µL) in four brain regions: hippocampus, dorsal striatum, primary somatosensory cortex (S1) and primary visual cortex (V1) (Fig. 2a). We analyzed brains 12–14 days post-injection to allow time for tdTomato protein expression and accumulation in genome-edited cells.

In vivo genome-editing was observed for both the 4xNLS-Cas9–2xNLS and 0xNLS-Cas9–2xNLS RNPs that targeted tdTomato, but not for RNPs loaded with non-targeting sgRNA, showing RNP specificity. Similar to *in vitro* results, the 4xNLS-Cas9–2xNLS RNP was 10-fold more efficient at editing cells in the brain compared to the 0xNLS-Cas9–2xNLS RNP in all four brain regions tested (Fig. 2b).

We next performed dual color immunofluorescence to identify the cell-types that 4xNLS-Cas9–2xNLS RNP edits *in vivo*. In the cortex, tdTomato⁺ cells co-localized with NeuN (post-mitotic neuronal marker). In the hippocampus, tdTomato⁺ cells co-localized with CTIP2 (also known as BCL11a), a transcription factor present in CA1 hippocampus and striatal post-mitotic neurons. Interestingly, in the hippocampus tdTomato⁺ cells did not co-localize with GFAP, an astrocyte marker protein. In the striatum, tdTomato⁺ cells co-localized with CTIP2 and DARPP-32 (cAMP-regulated neuronal phosphoprotein), a well-documented marker of GABAergic striatal medium spiny neurons. As in the hippocampus, genome-editing was not detected in astrocytes as there was no tdTomato⁺ co-localization with GFAP nor S100β, (a protein highly expressed in striatal astrocytes) (Fig. 2c). Therefore our cellular analysis showed 4xNLS-Cas9–2xNLS RNP-mediated editing of diverse neuronal subtypes and not astrocytes.

To investigate whether increased dose of 4xNLS-Cas9–2xNLS RNP would increase the number or volume of genome-edited cells, we performed a 4, 15 and 30pmol RNP per 0.5µl intrastriatal injection dose course. We observed significantly more tdTomato⁺ cells with increasing RNP dose, 4pmol (588 ±90 cells), 15pmol (1339 ±331 cells), 30pmol (2675 ±613 cells), 4pmol vs. 30pmol (p=0.0188) (Fig. 2e,f). We noted the highest RNP dose (30pmol) had a 3-fold larger volume of tdTomato⁺ tissue compared to the lowest RNP dose (4pmol), ~1.5mm³ vs. ~1mm³ (Supplementary Fig. 4). Since the same injection volume was used for each RNP dose, this result hints at a volume-independent mechanism of RNP spreading through the striatum interstitial space. We also observed increased density of tdTomato⁺ edited cells in the 30pmol Cas9 RNP (Fig. 2e and Supplementary Fig. 4c). Notably, the efficiency of 4xNLS-Cas9–2xNLS RNP-mediated genome editing was ~100 tdTomato⁺ cells per pmol of RNP delivered and was not significantly different across the three RNP doses (p = 0.213) (Fig. 2g). This suggests calculating the amount of RNP needed to edit a given number of neurons could be possible (Supplementary Fig. 5).

To assess if there is an innate immune response to Cas9 RNP injected into the dorsal striatum, we analyzed activation of microglia, CNS resident immune cells, by IBA-1

immunostaining and relative transcript expression of a panel of immune marker genes by qPCR (Supplementary Table 2). We did not observe significant IBA-1 intensity differences nor morphological differences among uninjected, sham injected and RNP injected brains, and qPCR of immune-related transcripts suggests an undetectable to mild microglia-mediated innate immune response following Cas9 RNP injection (Supplementary Fig. 6). The increased TNF-alpha transcript levels at 12 days post-injection could reflect an adaptive response to RNP delivery that reduces synaptic strength of the corticostriatal pathway for neuroprotection²⁴ and not an innate immune response. Future studies will explore this possibility.

Overall, our findings demonstrate efficient Cas9 RNP-mediated genome editing of neural progenitor cells *in vitro* and neurons in distinct brain regions *in vivo*. Although the mechanism of 4xNLS-Cas9–2xNLS RNP *in vivo* neuro-tropism is not yet understood, it can be exploited for neuron-specific targeting. Therefore this technology has the potential to be applied to treat genetic neurological diseases that manifest in distinct populations of neurons. The evidence that functional Cas9 RNPs can be effectively, precisely and safely delivered to neurons in the brains of adult animals in a non-genetically encoded manner has implications for future therapeutic use of Cas9 RNP complexes to treat neurological disease and for tissue-specific editing in general.

Online methods

Neural Progenitor cell (NPCs) line creation

NPCs were isolated from cortices from Embryonic Day 13.5 Ai9-tdTomato homozygous mouse embryos¹⁷. Cells were cultured as neurospheres in NPC Medium: DMEM/F12 with glutamine, Na-Pyruvate, 10mM HEPES, Non-essential amino acid, Pen/Strep (100X), 2-mercaptoethanol (1000X), B-27 without vitamin A, N2 supplement, bFGF and EGF, both 20ng/ml as final concentration. NPCs were passaged using MACS Neural Dissociation Kit (Papain) cat# 130-092-628 following manufacturers protocol. bFGF and EGF were refreshed every other day and passaged every six days. The NPC line was authenticated by immunocytochemistry marker protein staining. They were tested for mycoplasma using Hoechst stain with visual analysis and were negative.

Cas9 RNP direct delivery

Direct delivery RNP in NPC experiments was added to media and incubated with cells for 24 hours, then cells were washed 2x with 200U/ml Heparin in DMEM media and allowed to grow for 24 additional hours.

HEK293T-EGFP-PEST cell line creation

The d2EGFP reporter construct was created in a modified lentivirus backbone with EF1-a promoter driving the gene of interest and a second PGK promoter driving production of a gene which confers resistance to hygromycin. The EGFP is destabilized by fusion to residues 422–461 of mouse ornithine decarboxylase, giving an *in vivo* half-life of ~2 hours. Transduced 293T cells were selected with hygromycin (250 ug/ml). d2EGFP clones were isolated by sorting single cells into 96 well plates and characterized by intensity of d2EGFP.

Lentivirus was produced by PEI (Polysciences Inc., 24765) transfection of 293T cells with gene delivery vector co-transfected with packaging vectors pspax2 and pMD2.G essentially as described by. The parental HEK293T cell line was obtained from UC Berkeley Scientific Facilities and authenticated using STR analysis by DDCM. They were tested for mycoplasma using Hoechst stain with visual analysis and were negative.

HEK 293T EGFP disruption assay

GFP disruption assays were based on those previously described²⁵. HEK-293T-d2EGFP cells were used in these experiments because they are efficiently transfected with Cas9-RNP mixed with lipofectamine2000 and therefore useful for this experiment which analyzes the activity of our 0xNLS- and 4xNLS-Cas9-2xNLS RNPs post cell penetration. Briefly, HEK293T-d2EGFP cells were cultured in 10cm dishes using Dulbecco's Modification of Eagle's Medium (DMEM) with 4.5g/L glucose L-glutamine & sodium pyruvate (Corning cellgro) plus 10% fetal bovine serum, 1x MEM Non-Essential Amino Acids Solution (Gibco) and Pen-Strep (gibco). One day before transfection, $\sim 3 \times 10^4$ cells were plated into each well of a 96 well plate with the DMEM medium plus hygromycin and allowed to settle. The next day Cas9 RNP was complexed with Lipofectamine 2000 (Life Technologies) at 0.005–50pmol RNP+ 1 μ l Lipofectamine in 20ul OMEM media and added to the cells. Cells were analyzed for EGFP expression at 48 hours post transfection using a BD LSR Fortessa High-throughput sequencer.

NaCl hypertonic protein transduction

RNP's were added to NaCl hypertonic protein transduction solution: "CRISPR/Cas9 Transduction Media": Opti-MEM media (Life Technologies) supplemented with 542 mM NaCl, 333 mM GABA, 1.673 N2, 1.673 B27 minus vitamin A, 1.673 non-essential amino acids, 3.3 mM Glutamine, 167 ng/ml bFGF2, and 84 ng/ml EGF²³. This mixture was added to NPCs that were plated 1 day before at 9×10^4 cells per well of 96 well plate. The CRISPR/Cas9 Transduction Media + Cas9 RNPs were removed after 1 hour and replaced with growth media. Editing efficiency was assessed by FACS and genomicDNA PCR analysis.

Primary neuron culture

E18.5 cortical neurons were dissociated with MACS Neural Dissociation Kit (Papain) cat# 130-092-628 following manufacturers protocol. Cells were seeded in NBActive media (Brainbits) at 1500 cells/mm² on poly-ornithine, fibronectin, laminin coated, imaging quality, 96 well plates (Greiner Bio One). DIV4, 1/3 media change, DIV8, 1/3 media change, add RNP or RNP+Lipofectamine2000. Per well: 0.5ul Lipofectamine2000 + 5ul OMEM, incubate 10min at room temp. Add to (10pmol RNP + 5ul OMEM), incubate 10 min at room temp, add to cells. Incubate 16hours. Remove media and add pre-equilibrated, 50% conditioned media.

Cas9 purification

The recombinant *S. pyogenes* Cas9 used in this study carries two C-terminal SV40 nuclear localization sequences. The protein was expressed with an N-terminal hexahistidine tag and

maltose binding protein in *E. coli* Rosetta 2 cells (EMD Millipore, Billerica, MA) from plasmids based on pMJ915 (Addgene plasmid # 69090)¹⁴. N-terminal nuclear localization sequence peptide arrays and sfGFP modifications were cloned into the plasmid using Gibson DNA assembly technique (Supplementary Table 1). The His tag and maltose binding protein were cleaved by TEV protease, and Cas9 was purified by the protocols described previously³. Cas9 was stored in “Buffer 5” : 20mM 2-[4-(2-hydroxyethyl)piperazin-1-yl]ethanesulfonic acid (HEPES) at pH 7.5, 150 mM KCl, 10% glycerol, 1 mM tris(2-chloroethyl) phosphate (TCEP) and stored at -80°C . For *in vivo* experiments, Cas9 was buffer exchanged into “Buffer#1” (25 mM Na phosphate pH 7.25, 300 mM NaCl, 200 mM trehalose) before size exclusion column chromatography and stored at -80°C . Cas9 protein endotoxin levels were measured using Pierce LAL Chromogenic Endotoxin Quantification Kit Cat. # 88282.

sgRNA target site prediction

sgRNA target sequences were selected using the website <http://crispr.mit.edu>.²⁶

In vitro T7 transcription of sgRNA

The DNA template encoding: T7 promoter, a 20 nt target sequence and an optimized sgRNA scaffold²⁷ was assembled from synthetic oligonucleotides (Integrated DNA Technologies, San Diego, CA) by overlapping PCR. Target sequences are: sgRNA-tdTom aka sgRNA298 (targets STOP cassette in tdTomato locus), 5'-AAGTAAAACCTCTACAAATG-3', sgRNA-non-targeting aka sgRNA339 (targets Gal4 sequence that is not present in mouse genome), 5'-AACGACTAGTTAGGCGTGTA-3', sgRNANT3 (targets EGFP gene) 5'-GGTGGTGCAGATGAACTTCA-3'. Briefly, for the sgRNA-tdTom template, the PCR reaction contains 20 nM premix of BS298 (5'-TAA TAC GAC TCA CTA TAG AAG TAA AAC CTC TAC AAA TGG TTT AAG AGC TAT GCT GGA AAC AGC ATA GCA AGT TTA AAT AAG G-3') and BS6 (5'-AAA AAA AGC ACC GAC TCG GTG CCA CTT TTT CAA GTT GAT AAC GGA CTA GCC TTA TTT AAA CTT GCT ATG CTG TTT CCA GC -3'), 1 μM premix of T25_long (5'-GAA ATT AAT ACG ACT CAC TAT AG -3') and BS7 (5'-AAA AAA AGC ACC GAC TCG GTG C -3'), 200 μM dNTP and Phusion Polymerase (NEB, Ipswich, MA) according to the manufacturer's protocol. The thermocycler setting consisted of 40 cycles of 95°C for 10 s, 59°C for 10 s and 72°C for 10 s. The PCR product was extracted once with phenol:chloroform:isoamyl alcohol and then once with chloroform, before isopropanol precipitation overnight at -20°C . The DNA pellet was washed three times with 70% ethanol, air-dried and resuspended in Elution Buffer.

A 400- μl T7 *in vitro* transcription reaction consisted of 50 mM Tris-HCl (pH 8), 30 mM MgCl_2 , 0.01% Triton X-100, 2 mM spermidine, 20 mM fresh dithiothreitol, 5 mM of each ribonucleotide triphosphate, 100 $\mu\text{g}/\text{ml}$ T7 Polymerase and 1 μM DNA template. The reaction was incubated at 37°C for 4hr-to-overnight, and 5 units of RNase-free DNaseI (Promega, Madison, WI) was added to digest the DNA template 37°C for 1 hr. The reaction was quenched with 2xSTOP solution (95% deionized formamide, 0.05% bromophenol blue and 20 mM EDTA) at 60°C for 5 min. The RNA was purified by electrophoresis in 10% polyacrylamide gels containing 6 M urea. The RNA band was excised from the gel, crushed in a 15-ml tube, and eluted with 5 volumes of 300 mM sodium acetate (pH 5) overnight at

4°C. The supernatant was filtered through a 0.2µm filter to remove acrylamide fragments. 2.5 equivalents of ethanol was added and the RNA precipitated overnight at –20°C. The RNA pellet was collected by centrifugation, washed three times with 70% ethanol, and briefly air-dried or vacuum-dried. To refold the sgRNA, the RNA pellet was re-dissolved in dPBS-Ca,-Mg. The sgRNA was heated to 70°C for 5 min and cooled to room temperature for 5 min. MgCl₂ was added to a final concentration of 1 mM. The sgRNA was again heated to 50°C for 5 min, cooled to room temperature for 5 min and kept on ice. The sgRNA concentration was determined by OD_{260nm} using Nanodrop (Thermo Fisher Scientific, Waltham, MA). The sgRNA was stored at –80°C.

Cas9 RNP assembly

Cas9 RNP either was prepared immediately before experiments or prepared and snap-frozen in liquid nitrogen and stored at –80°C for later use. We did not measure any loss in activity upon freeze-thawing Cas9 RNP complexes. To prepare the Cas9 RNP complexes, we incubated Cas9 protein with sgRNA at 1:1.2 molar ratio. Briefly, we added sgRNA to Buffer#1 (25mM NaPi, 150mM NaCl, 200mM trehalose, 1mM MgCl₂), then added the Cas9 to the sgRNA, slowly with swirling, and incubated at 37°C for 10 min to form RNP complexes. RNP complexes were filtered prior to use through a 0.22µm Costar 8160 Filter pre-wet with 200µl Buffer#1. If needed, the RNP sample was concentrated with a 0.5ml Millipore Ultra 100Kd cutoff filter, part # UFC510096, until the desired volume was obtained.

Cas9 Nucleofection

Neural Progenitor Cell neurospheres were dissociated by the MACS Neural Dissociation Kit (Papain) cat# 130-092-628, spun down by centrifugation at 80×*g* for 3 min, and washed once with dPBS-Ca,-Mg. Nucleofection of NPCs with Cas9 RNP was performed using Lonza (Allendale, NJ) P3 cell kits and program EH-100 in an Amaxa 96-well Shuttle system. Each nucleofection reaction consisted of approximately 2.5×10^5 cells in 20 µl of nucleofection reagent and mixed with 10 µl of RNP. After nucleofection, 70 µl of growth media was added to the well to transfer the cells to tissue culture plates. For plasmid nucleofection, we used a modified pX330-U6-Chimeric_BB-CBh-hSpCas9 vector (Addgene plasmid # 42230¹ that contained the puromycin N-acetyltransferase (PuroR) gene and optimized sgRNA scaffold²⁷. Nucleofection was performed using 700 ng plasmid with 4×10^5 NPCs and Lonza P3 cell kit and program DS-113 in an Amaxa 96-well Shuttle system. The cells were incubated at 37°C for 1–5 days depending on the assay. For genomic DNA analysis the media was removed by aspiration, and 100 µl of Quick Extraction solution (Epicentre, Madison, WI) was added to lyse the cells (65°C for 20 min and then 95°C for 20 min) and extract the genomic DNA. The cell lysate was stored at –20°C. The concentration of genomic DNA was determined by NanoDrop. tdTomato activation in NPCs were analyzed by flow cytometry. UC Berkeley FACS Core facilities were used.

Animals

Mice were maintained on a 12 h light dark cycle with *ad libitum* access to food and water. All animals were group housed and experiments were conducted in strict adherence to the Swiss federal ordinance on animal protection and welfare as well as according to the rules of

the Association for Assessment and Accreditation of Laboratory Animal Care International (AAALAC), and with the explicit approval of the local veterinary authorities. Animals at University of California, Berkeley were maintained on a 12 h light dark cycle with *ad libitum* access to food and water. All animals were group housed and experiments were conducted in strict adherence to the University of California, Berkeley's Animal Care and Use Committee (ACUC) ethical regulations. No randomization was used to allocate animals to experimental groups.

Stereotaxic infusion of Cas9 RNP's

0xNLS-Cas9–2xNLS and 4xNLS-Cas9–2xNLS RNPs were prepared and shipped by Brett Stahl, UC Berkeley to Roche Pharmaceuticals Basel, Switzerland. 15 – 20 weeks old male Ai14 tdTomato mice (which lack the NeoR cassette present in Ai9 tdTomato mice but are otherwise identical)¹⁷ were anesthetized using injectable anesthesia (Fentanyl 0.05 mg/Kg + Medetomidine 0.5 mg/kg + Midazolam 5 mg/kg; s.c.). The anesthetized mouse was then aligned on an Angle two stereotaxic frame (Leica, Germany) and craniotomies were performed with minimal damage to brain tissue. All stereotaxic coordinates are relative to bregma. Mouse stereotaxic surgery targets: striatum (+0.74 mm anteroposterior, ±1.74 mm mediolateral, –3.37 mm dorsoventral), hippocampus (–1.94 mm anteroposterior, ±1.12 mm mediolateral, –1.75 mm dorsoventral), cortex V1 (–3.28 mm anteroposterior, ±2.4 mm mediolateral, –1.25 mm dorsoventral), cortex S1 (+1.94 mm anteroposterior, ±2.37 mm mediolateral, –2.00 mm dorsoventral). Cas9 RNPs were infused (0.5µl/side) using a Neuros 75 5µL syringe (Hamilton). After infusion, the injector was left at the injection site for 5 min and then slowly withdrawn. After the injections, the operation field was cleaned with sterile 0.9% NaCl and closed with suture (Faden Monocryl Plus 5–0, Aichele Medico) and surgical glue (3M™ Vetbond™ Tissue Adhesive). The mouse was kept warm at 37°C during the surgical procedure and also post-surgery. To avoid drying of the eyes during surgery, an ointment was applied outside of the eyes of the mouse. The mice were left undisturbed for 12 days before cellular analysis. Sample size was chosen based on expected effect size. No randomization was applied while allocating animals to groups.

Immunofluorescence analysis

For immunofluorescence analysis, mice were perfused with 4% paraformaldehyde and post-fixed overnight. Brains were sectioned (coronal plane sections) on a vibratome and 50 µm thick sections were used for antibody labeling. Sections were first treated with blocking solution (0.3% Triton X-100, 10% goat serum in 1X PBS) and incubated with the primary antibody (in blocking solution) overnight at 4 °C. Sections were washed with 1X PBS and incubated in the secondary antibody at room temperature for 3 hours. Finally, sections were washed three times in 1X PBS, stained with the DNA binding fluorescence probe DAPI (1 µg/ml, Roche Life Science, Switzerland) and mounted on glass slides in a Prolong gold anti-fade medium (Thermo Fischer, USA).

***In vivo* tdTomato reporter**

For tdTomato reporter analysis, 12–14 days post injection mice were perfused with 4% paraformaldehyde and brains were post-fixed overnight. Brains were sectioned (coronal

plane sections) on a vibratome and 50 μm thick sections were DAPI counterstained and endogenous tdTomato⁺ cells counted.

Primary antibodies (Supplementary Table 3) used are polyclonal rabbit anti-IBA1 (1:100, Wako, #019–19741), polyclonal rabbit anti-S100 β (1:1000; Abcam, # ab41548), monoclonal rabbit anti-DARPP32 (1:100, Cell signaling technologies, # 2306), monoclonal mouse anti-NeuN (1:500; Millipore, #MAB377), Polyclonal chicken anti-GFAP (1:500; Abcam, # ab4674), and monoclonal rat anti-CTIP2 (1:100; clone 25B6, Abcam, # ab18465). Secondary antibodies used are donkey anti-rabbit Alexa Fluor 488 (1:500, Jackson Lab, USA, #711-545-152), and donkey anti-rat Alexa Fluor 488 (1:500, Thermo Fischer, USA, #A-21208), donkey anti-chicken Alexa Fluor 488 (1:500; Jackson Labs, Bar Harbor, ME, #703-545-155), donkey anti-mouse Alexa Fluor 488 (1:500; Jackson Labs, Bar Harbor, ME, #715-545-150).

Confocal Imaging

Confocal fluorescent images were acquired using a Leica TCS SP5 (Leica Microsystems) inverted microscope. Image analysis and maximum intensity projections of images acquired along the z-axis was done using LAS-AF software.

Cell Counting

Images for cell counting were acquired using a Leica TCS SP5 (Leica Microsystems) inverted confocal microscope with 20x dry objective. Image analysis and maximum intensity projections of images acquired along the z-axis was done using LAS-AF software. Every sixth section from the dorsal striatum was stained with DAPI and used for cell counting. Quantification of Td-tomato and DAPI double positive cells was done using ImageJ. The total number of edited cells per brain was quantified by multiplying the number of cells counted with the section periodicity (here it is 6). The experimenter was blinded to treatment condition while performing cell counting.

Quantification of Fluorescence Intensity

Images for quantification were acquired a Leica TCS SP5 (Leica Microsystems) inverted microscope with 20x dry objective. All parameters were kept constant to allow comparative measurements between images. To quantify the fluorescence intensity corresponding to microglia (IBA-1 staining) at the injection site, we performed reconstruction of the injection site of the slice by recording at least 140 single optical layers (step size system optimized of 0.18 μm) at a 512–512 pixel resolution. The brightest sample was used to define optimal confocal settings with such settings used for the acquisition of all subsequent z stacks. LAS AF Lite software was used to reconstruct 3D Projection of the section. Quantification of the intensity of IBA-1 staining in the striatum was done with ImageJ Software. Data are represented as mean \pm SEM (One way ANOVA; $p = 0.4496$ and $F_{2,7} = 0.898$). $n=3$ animals per condition with 2–8 sections analyzed per animal. For each section, fluorescence intensity of the IBA-1 labeled channel for the entire 20X field was measured with image J. The experimenter was blinded to treatment condition while performing quantitation of fluorescence intensity.

RNA extraction from brain tissue slices and quantitative RT-PCR

Bilateral intrastriatal stereotaxic infusion of sham (buffer only) or 50pmol 4xNLS-Cas9–2xNLS RNPs with sgRNA-tdTomato in 0.5µl were performed as described earlier. Mice were perfused with ice cold PBS at 3 days and 12 days post injection. Brains were harvested and cut into 1mm sections using a brain slicer matrix around the injection site. The slices were transferred to ice-cold PBS and then onto frozen glass slides. The dorsal injected striatum (1mm thick x 1–1.25mm wide x 2mm long) was cut out and frozen on dry ice. On Day3, tdTomato+ signal was not yet present so we therefore identified the needle track to excise the RNP treated tissue in the dorsal striatum. On day 12, tdTomato+ signal accumulated in edited cells, and we used the needle track in addition to the tdTomato signal to identify RNP treated tissue in the dorsal striatum. One milliliter of TRIzol reagent (Invitrogen) was added to 50mg (3 day) or 150mg (12 day) of tissue and triturated to dissociate tissue. One microgram of total RNA was treated with DNase I to remove potential contamination of genomic DNA. One microgram of DNase I-treated RNA was reverse transcribed using a First Strand Synthesis kit (Invitrogen). qRT-PCR analysis was performed using SYBR green master mix on a Applied Biosystems Step One Plus. The relative expression from RNA samples was determined using the 2^{-CT} method. Values were normalized to the expression of the PPIA housekeeping gene. Error bars represent SEM. n=3 animals, n=2 injections per animal for each group. To test the statistical significance of observed gene expression differences, we performed two-tailed unpaired t tests with equal SD. Primers are listed in Supplementary Table 2. Sample size was chosen based on expected effect size. No randomization was applied while allocating animals to groups. The experimenter was blinded to treatment condition while collecting tissue.

NexGen Sequence Analysis

The genomic region flanking the CRISPR target site was amplified by 2-step PCR method using primers listed in Supplementary Fig 2a. First, the genomic DNA from the edited and control samples was isolated and PCR amplified 15 cycles using Kapa Hot start high-fidelity polymerase (Kapa Biosystems, Wilmington, MA) according to the manufacturer's protocol. The resulting amplicons were purified by AMPure beads to remove primers and subjected to five cycles of PCR to attach Illumina P5 adapters as well as unique sample-specific barcodes followed by bead purification. Berkeley Sequencing facility performed the AMPure bead cleanup. Barcoded and purified DNA samples were quantified by Qubit 2.0 Fluorometer (Life Technologies, Carlsbad, CA), size analyzed by BioAnalyzer, quantified by qPCR and pooled in an equimolar ratio. Sequencing libraries were sequenced with the Illumina MiSeq Personal Sequencer (Life Technologies, Carlsbad, CA). Amplicon sequencing data were analyzed with CRISPR-GA²⁸. This work used the Vincent J. Coates Genomics Sequencing Laboratory at UC Berkeley.

Supplementary Material

Refer to Web version on PubMed Central for supplementary material.

Acknowledgements

We thank L. Harrington, T. Gaj, S. Lin, R. Rouet, C. Fellmann and D. Schaffer for productive discussions and comments on the manuscript as well as L. Bai for technical support. This work was supported by a F. Hoffmann-La Roche Postdoctoral Fellowship, RPF311, award to B.T.S. and by a Roche Pharmaceutical's Roche Alliance with Distinguish Scientists (ROADS) Fund award to J.A.D. J.A.D. is an HHMI Investigator and a Paul Allen Frontiers in Science investigator. M.B. and C.C.B. are employed by F. Hoffmann-La Roche. A.G. was employed by F. Hoffmann-La Roche during the time of this study.

References

1. Cong L et al. Multiplex genome engineering using CRISPR/Cas systems. *Science* 339, 819–823 (2013). [PubMed: 23287718]
2. Mali P et al. CAS9 transcriptional activators for target specificity screening and paired nickases for cooperative genome engineering. *Nat Biotechnol* 31, 833–838 (2013). [PubMed: 23907171]
3. Jinek M et al. A Programmable Dual-RNA-Guided DNA Endonuclease in Adaptive Bacterial Immunity. *Science* 337, 816–821 (2012). [PubMed: 22745249]
4. Jinek M et al. RNA-programmed genome editing in human cells. *eLife* 2, e00471–e00471 (2013). [PubMed: 23386978]
5. Zuris JA et al. Cationic lipid-mediated delivery of proteins enables efficient protein-based genome editing in vitro and in vivo. *Nat Biotechnol* (2014). doi:10.1038/nbt.3081
6. Yin H et al. Genome editing with Cas9 in adult mice corrects a disease mutation and phenotype. *Nat Biotechnol* (2014). doi:10.1038/nbt.2884
7. Nelson CE et al. In vivo genome editing improves muscle function in a mouse model of Duchenne muscular dystrophy. *Science* 351, 403–407 (2016). [PubMed: 26721684]
8. Long C et al. Postnatal genome editing partially restores dystrophin expression in a mouse model of muscular dystrophy. *Science* 351, 400–403 (2016). [PubMed: 26721683]
9. Tabebordbar M et al. In vivo gene editing in dystrophic mouse muscle and muscle stem cells. *Science* 351, 407–411 (2016). [PubMed: 26721686]
10. Wu W-H et al. CRISPR Repair Reveals Causative Mutation in a Preclinical Model of Retinitis Pigmentosa. 1–7 (2016). doi:10.1038/mt.2016.107
11. Chew WL et al. A multifunctional AAV-CRISPR-Cas9 and its host response. *Nat Meth* 13, 868–874 (2016).
12. Ran FA et al. Genome engineering using the CRISPR-Cas9 system. *Nature Protocols* 8, 2281–2308 (2013). [PubMed: 24157548]
13. Kim S, Kim D, Cho SW, Kim J & Kim J-S Highly efficient RNA-guided genome editing in human cells via delivery of purified Cas9 ribonucleoproteins. *Genome Research* 24, 1012–1019 (2014). [PubMed: 24696461]
14. Lin S, Stahl BT, Alla RK & Doudna JA Enhanced homology-directed human genome engineering by controlled timing of CRISPR/Cas9 delivery. *eLife* 3, e04766 (2014). [PubMed: 25497837]
15. Woo JW et al. DNA-free genome editing in plants with preassembled CRISPR-Cas9 ribonucleoproteins. *Nat Biotechnol* 1–4 (2015). doi:10.1038/nbt.3389 [PubMed: 25574611]
16. Wang M et al. Efficient delivery of genome-editing proteins using bioreducible lipid nanoparticles. *Proc. Natl. Acad. Sci. U.S.A.* 113, 2868–2873 (2016). [PubMed: 26929348]
17. Madisen L et al. A robust and high-throughput Cre reporting and characterization system for the whole mouse brain. *Nat. Neurosci* 13, 133–140 (2009). [PubMed: 20023653]
18. Ramakrishna S et al. Gene disruption by cell-penetrating peptide-mediated delivery of Cas9 protein and guide RNA. *Genome Research* gr.171264113 (2014). doi:10.1101/gr.171264.113
19. Dokka S, Toledo D, Shi X, Castranova V & Rojanasakul Y Oxygen radical-mediated pulmonary toxicity induced by some cationic liposomes. *Pharm. Res* 17, 521–525 (2000). [PubMed: 10888302]
20. Armeanu S Optimization of Nonviral Gene Transfer of Vascular Smooth Muscle Cells in Vitro and in Vivo. *Molecular Therapy* 1, 366–375 (2000). [PubMed: 10933955]

21. Liu J, Gaj T, Wallen MC & Barbas CF Improved Cell-Penetrating Zinc-Finger Nuclease Proteins for Precision Genome Engineering. 1–9 (2015). doi:10.1038/mtna.2015.6
22. Pédelacq J-D, Cabantous S, Tran T, Terwilliger TC & Waldo GS Engineering and characterization of a superfolder green fluorescent protein. *Nat Biotechnol* 24, 79–88 (2005). [PubMed: 16369541]
23. D'Astolfo DS et al. Efficient Intracellular Delivery of Native Proteins. *Cell* 161, 674–690 (2015). [PubMed: 25910214]
24. Lewitus GM, Pribiag H, Duseja R, St-Hilaire M & Stellwagen D An adaptive role of TNF α in the regulation of striatal synapses. *Journal of Neuroscience* 34, 6146–6155 (2014). [PubMed: 24790185]
25. Gilbert LA et al. CRISPR-Mediated Modular RNA-Guided Regulation of Transcription in Eukaryotes. *Cell* 154, 442–451 (2013). [PubMed: 23849981]
26. Hsu PD et al. DNA targeting specificity of RNA-guided Cas9 nucleases. *Nat Biotechnol* 31, 827–832 (2013). [PubMed: 23873081]
27. Chen B et al. Dynamic Imaging of Genomic Loci in Living Human Cells by an Optimized CRISPR/Cas System. *Cell* 155, 1479–1491 (2013). [PubMed: 24360272]
28. Güell M, Yang L & Church GM Genome editing assessment using CRISPR Genome Analyzer (CRISPR-GA). *Bioinformatics* 30, 2968–2970 (2014). [PubMed: 24990609]
29. Chen Z et al. Microglial displacement of inhibitory synapses provides neuroprotection in the adult brain. *Nature Communications* 5, 1–12 (1AD).

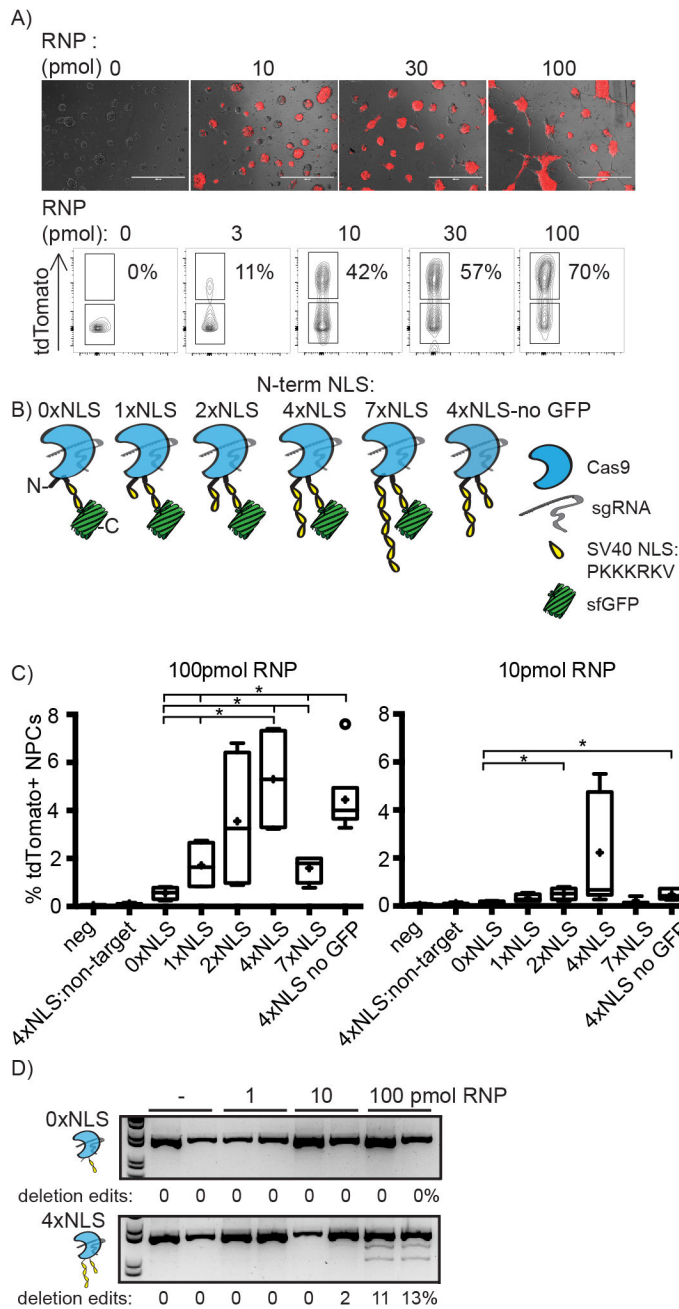


Figure 1. Generation of cell penetrating Cas9 RNPs.

A) Images and flow cytometry analysis of *tdTomato*⁺ NPC neurospheres 3 days post-nucleofection of Cas9 RNP dose course. Scale bar 400 μ m. Representative data from n=3 independent experiments. B) N-terminal 1–7xNLS-Cas9–2xNLS design; C) Direct delivery of 1–7xNLS-Cas9–2xNLS with NPCs led to activation of *tdTomato* reporter in genome-edited cells. 4xNLS-Cas9–2xNLS designs are more efficient at genome-editing cells than other designs. Data are represented as Tukey box and whisker plots, box is IQR, whiskers are the lowest datum still within 1.5 IQR of the lower quartile, and the highest datum still within 1.5 IQR of the upper quartile, outliers are open circles, + is mean, line in

median(100pmol 0xNLS vs. 4xNLS; Two-tailed Unpaired t test with Welch's correction; $p = 0.0236$ and $F_{3,3} = 80.50$. 100pmol 0xNLS vs. 4xNLS-noGFP; Two-tailed Unpaired t test with Welch's correction; $p = 0.0015$ and $F_{5,3} = 39.04$. 100pmol 1xNLS vs. 4xNLS-noGFP; Two-tailed Unpaired t test with Welch's correction; $p = 0.0099$ and $F_{5,3} = 2.434$. 100pmol 0xNLS vs. 7xNLS; Two-tailed Unpaired t test with Welch's correction; $p = 0.0283$ and $F_{3,3} = 5.246$. 10pmol 0xNLS vs. 2xNLS; Two-tailed Unpaired t test with equal SD; $p = 0.0096$ and $F_{2,2} = 2.597$. 10pmol 0xNLS vs. 4xNLS-noGFP; Two-tailed Unpaired t test with equal SD; $p = 0.0462$ and $F_{3,2} = 4.072$) $n=4$ experimental replicates with 2 technical replicates each. D) Genomic DNA PCR of tdTomato STOP locus validates tdTomato⁺ flow cytometry analysis. 4xNLS-Cas9-2xNLS RNP complexes yield deletion edits (lower 2 bands) while 0xNLS-Cas9-2xNLS RNP complexes do not. 100pmol 4xNLS-Cas9-2xNLS RNP bottom DNA band (activated *tdTomato* locus) contains 5.4% \pm 0.4% of the total DNA correlating with %tdTomato⁺ cells observed in 1C. Representative gel from $n=4$ experimental replicates with 2 technical replicates each.

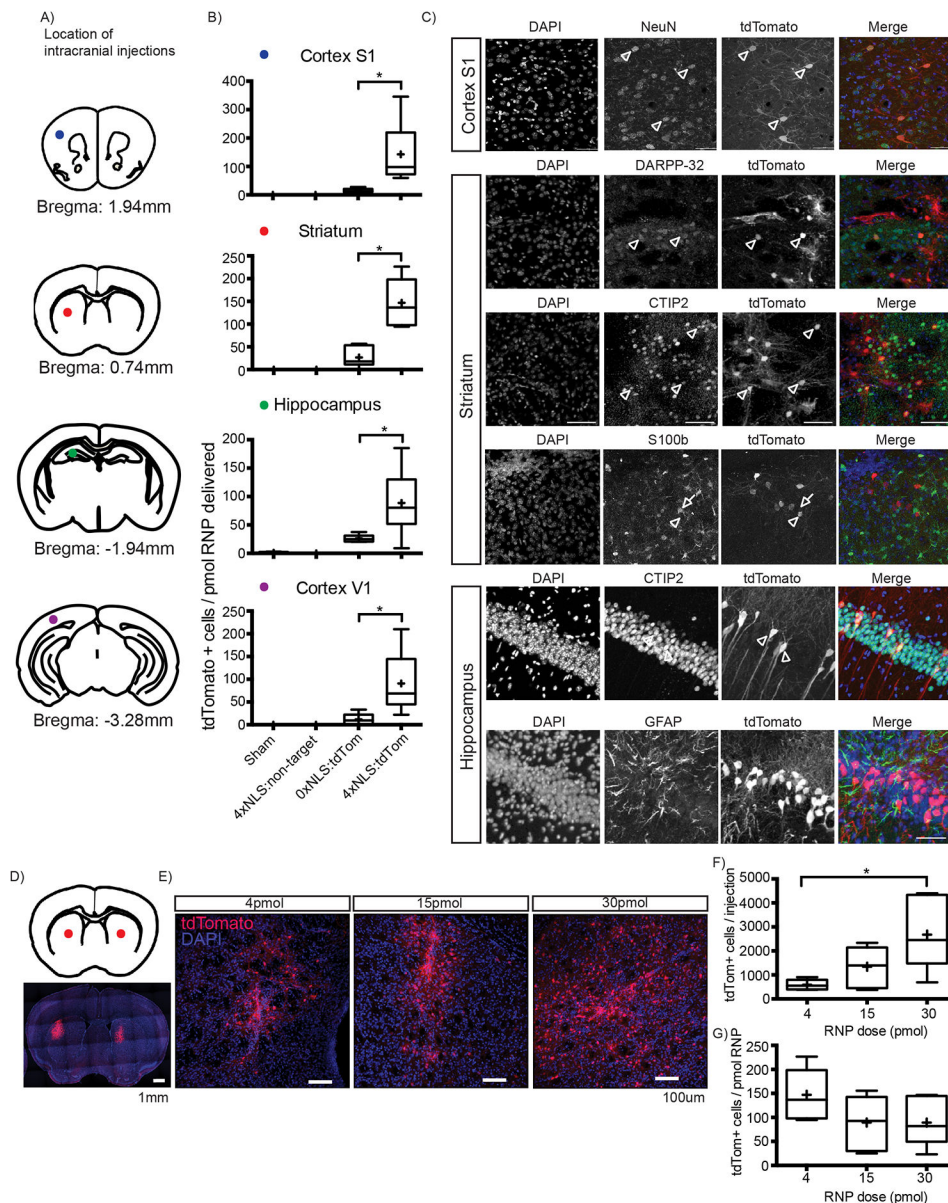


Figure 2. Injection of Cas9 RNP into multiple brain regions in adult mice

A) Color-coded dots indicate stereotaxic injection sites on coronal cartoons of mouse brain. Single Cas9 RNP injections (4pmol/0.5 μ l) with (Cas9 construct; sgRNA) 0xNLS-Cas9–2xNLS;sgRNA-tdTom, 4xNLS-Cas9–2xNLS;sgRNA-non-targeting, 4xNLS-Cas9–2xNLS;sgRNA-tdTom or sham (injection buffer only) into hippocampus, striatum, primary somatosensory cortex (S1), primary visual cortex V1. Male mice are 14–15 weeks old. B) Quantification of tdTomato⁺ cells / pmol RNP delivered. Brains were analyzed 12–14 days post injection. 50 μ m thick floating sections, 1 section every 300 μ m analyzed. 4xNLS-Cas9–2xNLS RNPs are significantly more efficient compared to 0xNLS-Cas9–2xNLS RNPs for *in vivo* genome-editing in all brain regions tested. Sham and 4xNLS-Cas9–2xNLS;non-targeting RNPs do not activate tdTomato indicating specificity of genome editing with Cas9 RNPs. Data are presented as mean \pm SEM (4xNLS;tdTom vs. 0xNLS;tdTom; Two-tailed

Unpaired t test with equal SD; $p = 0.002$ and $F_{5,5} = 5.9$ for the striatum. Two-tailed Unpaired t test with Welch's correction $p = 0.03$ and $F_{5,5} = 215$ for Cortex S1. $p = 0.03$ and $F_{5,5} = 25$ for Cortex V1. $p = 0.04$ and $F_{5,5} = 83$ for the hippocampus.) The sample size for each group is as follows: Sham and 4xNLS-Cas9-2xNLS;non-targeting: $n=2$ animals, $n=2$ injections per animal for each group, 0xNLS-Cas9-2xNLS;tdTom: $n=3$ animals, $n=2$ injections per animal, 4xNLS-Cas9-2xNLS;tdTom: $n=3$ animals, $n=2$ injections per animal. C) Representative confocal microscopy images of 4xNLS-Cas9-2xNLS RNP treated cells identify tdTomato⁺ cells co-localizing with neuron and not astrocyte marker proteins. NeuN, neuronal specific nuclear protein in vertebrates. CTIP2, aka BCL11a, a transcription factor present in CA1 hippocampus and striatum neurons. DARPP-32, cAMP-regulated neuronal phosphoprotein, a marker of striatum medium spiny neurons. GFAP, glial fibrillary acidic protein, an intermediate filament protein expressed in astrocytes and ependymal cells of the CNS. S100 β , a highly expressed protein in striatal astrocytes. Scale bar is 50 μ m. D) Increasing dose of 4xNLS-Cas9-2xNLS RNP significantly increases number of tdTomato⁺ genome-edited cells in the striatum. Red dots indicate bilateral stereotaxic injection sites on coronal cartoon of mouse brain. Coronal section mosaic tile image of bilateral 30pmol RNP injections with tdTomato reporting genome-editing in the striatum. Blue=DAPI staining nuclei, Red=endogenous tdTomato expression. E) Representative confocal images of tdTomato⁺ cells in single 4, 15, 30pmol/0.5 μ l injection dose course. Scale bar 100 μ m. F) Quantification of total # tdTomato⁺ cells per injection site. Data are presented as Tukey box and whisker plots. Box is IQR, whiskers are the lowest datum still within 1.5 IQR of the lower quartile, and the highest datum still within 1.5 IQR of the upper quartile, + is mean, line is median Two-tailed Unpaired t test with Welch's correction $p = 0.0188$ and $F_{5,5} = 46.03$ for 4pmol v.30pmol. $p = 0.0536$ and $F_{5,5} = 13.43$ for 4pmol v. 15pmol. Two-tailed Unpaired t test with equal SD; $p = 0.0845$ and $F_{5,5} = 3.428$ for 15pmol v.30pmol. $n=3$ animals, $n=2$ injections per animal for each group. G) Quantification of tdTomato⁺ cells per pmol RNP delivered (1 tdTomato⁺ cell per 10fmol RNP). Data are presented as Tukey box and whisker plots. Box is IQR, whiskers are the lowest datum still within 1.5 IQR of the lower quartile, and the highest datum still within 1.5 IQR of the upper quartile, + is mean, line is median ($p = 0.213$; Kruskal-Wallis test. $n=3$ animals, $n=2$ injections per animal for each group).